

A Comparative Study of Different Type MPPT Technique for Solar (PV) System

Harsh Bhati

Dept. Electrical Engineering

Rajasthan Technical University, Kota

Kota, India

Harsh8bhati@gmail.com

Dr. Lata Gidwani (IEEE Member)

Dept. Electrical Engineering

Rajasthan Technical University, Kota

Kota, India

lgidwani@rtu.ac.in

Abstract

The three solar system's maximum power point tracking (MPPT) techniques Perturb and Observe (P&O), Incremental Conductance (InC), and a fuzzy logic-based tracking methodology are fully evaluated in this study. In the three techniques under investigation P&O, InC, and the FLC algorithm the operating point oscillates around the maximum power point during steady-state operation, causing energy loss from the output panel. This research highlights this problem in all three of these systems. Through simulation results, it is shown that the proposed fuzzy logic controller (FLC) offers more precise and rapid maximum power tracking than the other systems under discussion. This research sheds light on FLC's potential to improve solar system's efficiency and performance.

Keywords:-P&O, InC, FLC, MPPT, Solar PV System, Buck-Boost.

I. INTRODUCTION

Solar power stands as a promising alternative technology, offering hope of reducing our dependency on petroleum-based energy sources. However, the major challenge lies in the relatively poor efficiency of solar panel technology and its higher costs per kilo-watt-hour (kWh) compared to conventional petroleum energy sources[1]. At present, solar panels exhibit approximately 30% efficiency in converting sunlight into usable energy. Moreover, the charge controllers and other components within solar power systems also suffer from inefficiencies and high costs. To address this, our primary objective is to develop a specialized MPPT a charge controller designed to unlock the full potential of solar panels. By optimizing the solar panel's performance, we aim to enhance efficiency, reduce costs, and pave the way for solar power to become a more competitive and viable energy source in comparison to petroleum-based alternatives[2]. The MPPT is a crucial charge controller that modifies a solar cell's dynamic V-I characteristic. By manipulating the voltage and current output, the MPPT effectively enhances the power flow into the battery or batteries, even without physically altering the load[3]. Continuously monitoring the solar panel's output voltage and current, the MPPT intelligently identifies the optimal operating point that maximizes the power transferred to the batteries. Achieving precise tracking of this ever-changing operating point results in increased solar cell efficiency. Numerous algorithms have been developed to track the MPP of a photovoltaic (PV) generator[4][5]. The efficiency, complexity, rate of convergence, number of necessary sensors, and cost of these algorithms vary. This paper focuses on a detailed study of three MPPT methods: P&O, InC, and the FLC. Through this comparative analysis, we aim to identify the most efficient and cost-effective MPPT technique for enhancing the performance of solar power systems.

II. DESCRIPTION OF A PHOTOVOLTAIC SYSTEM

Figure 1 illustrates the solar cell's corresponding electrical circuit. It includes diodes, a source of current created by light, series resistance, and parallel resistance[6].

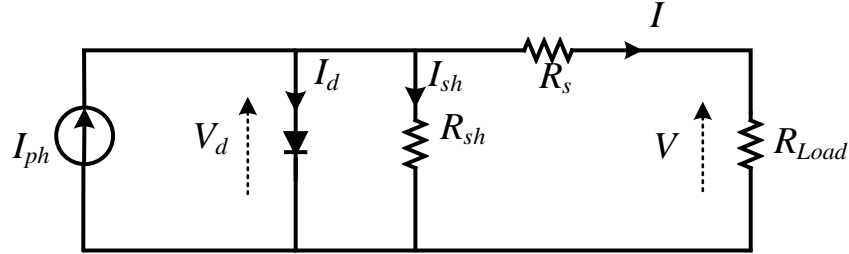


Figure 1: Solar cell equivalent electrical circuit

These are the current and voltage characteristic equations for solar cells:

$$I = I_{ph} - I_{sat} * \left[\exp\left(\frac{q * (V + RI)}{nkT}\right) - 1 \right] - \frac{V + RI}{R_{sh}} \quad (1)$$

where I is the current of a solar array (A), V is the output voltage of the array (V), I_{ph} is a light generation current (A), I_{sat} is the reverse saturation current of the diode (A), q is the electronic charge (C), p-n junction diode has a dimensionless deviation, which is called n , Boltzmann's constant is k (JK^{-1}), and so on. R_s refers to series resistance, R_{sh} is for shunt resistance, and T represents the cell temperature in Kelvins.

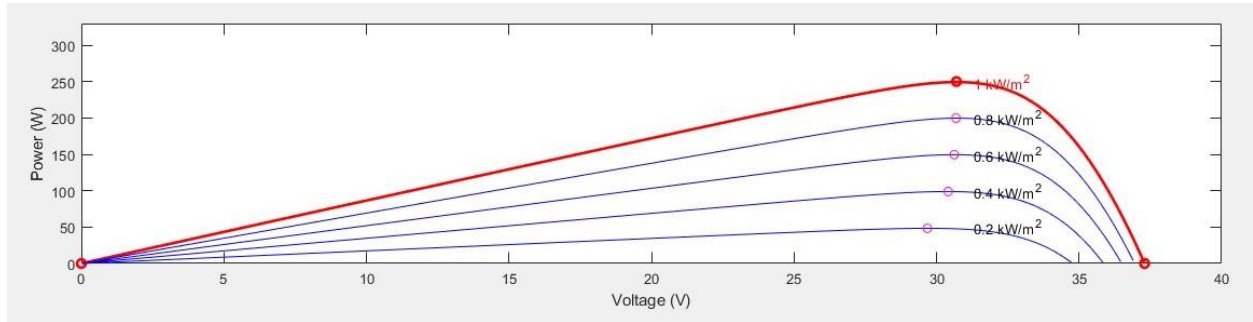


Figure 2: V-P characteristics of a photovoltaic panel for five different irradiance levels

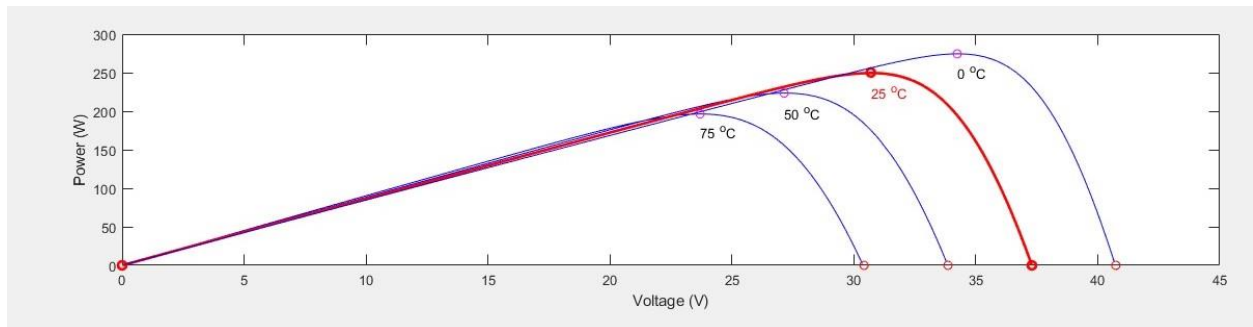


Figure 3: V-P characteristics of a photovoltaic panel for four different temperature levels

Figures 2 and 3 illustrate a photovoltaic module's P-V characteristics for a variety of irradiance and temperature values.

It is clear that the nonlinear output characteristics of the PV array are significantly influenced by solar radiation, temperature, and load conditions.

A solar module must be operated at a certain point with the proper voltage and current values and, to put it another way, at a specific load resistance to optimize output power. This needs a separate power converter circuit for the MPPT. In order to match the load to the PV array and extract maximum power, a BC (DC-DC) is used in our design.⁹

III. BOOST CONVERTER (DC-DC)

The BC power stage's construction is seen in Figure 4. It is made up of a boost inductor L , a load resistor R_{Load} , an output diode D , a filter capacitor C_2 , a power switch S (MOSFET transistor), and a filter capacitor C_2 . A particular kind of DC-DC converter called a BC has the ability to step up the input voltage to a greater output voltage. Since it functions in the continuous conduction mode, the boost inductor's current never completely zeroes out during a switching cycle. During the on-state of the switch K , the input voltage is applied to the boost inductor, and the current in the inductor increases linearly. The diode is in the off state during this time, preventing current flow through it. The boost inductor's energy is released when the switch K is switched off. The inductor tries to maintain current flow, and as the diode is now forward-biased, the inductor's energy is transferred to the output circuit ($R_{Load}C_2$) through the diode[7]. This process allows the load voltage to be higher than the source voltage. The switching action of the boost converter causes the output current to be pulsating. However, to obtain a stable DC voltage at the output, a capacitive filter is used. The capacitive filter smooths out the pulsating current, resulting in a more constant DC voltage being delivered to the load. To analyze the steady-state operation of the boost converter, we can derive its transfer function. The DC voltage transfer function represents the relationship between the output voltage and the input voltage of the converter. It can be obtained by considering the steady-state behavior of the circuit, which accounts for the effects of the inductor, diode, and capacitor in the continuous conduction mode. Without the specific values of the components and the control scheme, it is challenging to provide the exact transfer function formula. The transfer function depends on the specific circuit topology and its control strategy.

$$M(\delta) = \frac{V_o}{V_i} = \frac{-\delta}{1-\delta} \quad (2)$$

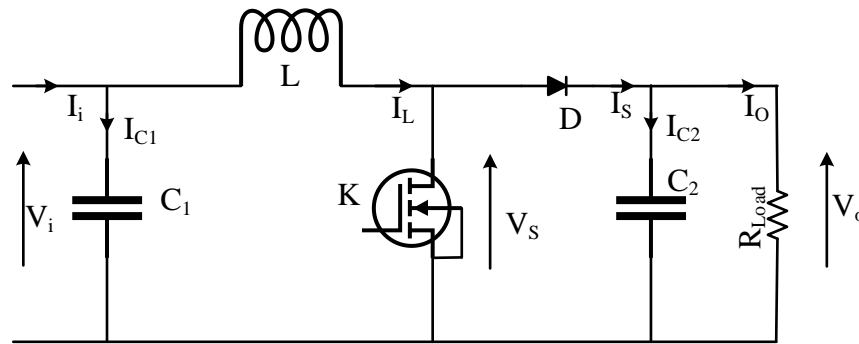


Figure 4: MPPT Boost Converter

IV. DIFFERENT MPPT ALGORITHMS

Effective operation of a photovoltaic power generation system relies on the capacity to accurately monitor the MPP under a variety of array temperatures and solar radiation conditions. As a consequence, continuing research and development has been done to build MPP control algorithms that can use the solar array's electricity as efficiently

as possible. Here, we conduct a thorough analysis using numerical simulations to assess the performance of three different MPP control methods. The objective is to determine the best-suited algorithm that guarantees the solar array's maximum performance and optimizes power production.

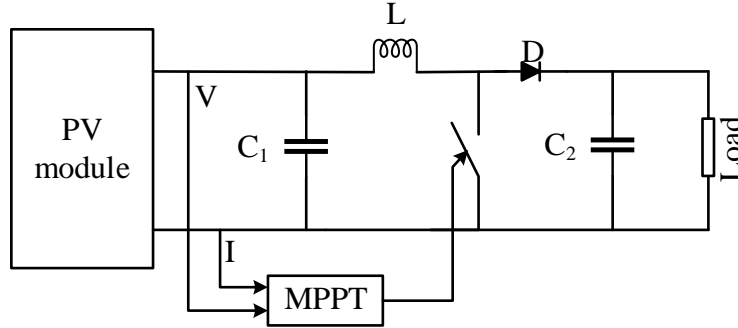


Figure 5: PV system with DC-DC Boost Converter, MPPT

A. Incremental conductance method

The basis for the InC approach is the fact that the following equation holds at the MPP:

$$\left(\frac{dI_{PV}}{dV_{PV}}\right) + \left(\frac{I_{PV}}{V_{PV}}\right) = 0 \quad (3)$$

I_{PV} and V_{PV} represent the PV array's current and voltage. When the operating point in the P-V plane is to the right of the MPP, $(dI_{PV}/dV_{PV}) + (I_{PV}/V_{PV}) < 0$, whereas when it is to the left, it is >0 [8]. Thus, the MPP may be tracked by comparing instantaneous I_{PV}/V_{PV} to incremental dI_{PV}/dV_{PV} . If $(dI_{PV}/dV_{PV}) + (I_{PV}/V_{PV})$ exceeds ϵ , it indicates a drop in power generation and indicates the direction of the MPP disturbance. When MPP is attained, PV array operation continues if dI_{PV} does not change, and perturbation ends. The algorithm adjusts the PV array voltage V_{PV} to meet a new MPP upwards or downwards. Increment size controls MPP tracking speed. The InC method works effectively in fast-changing weather. The classic IC approach requires measuring PV array voltage (V_{PV}) and current (I_{PV}) to determine perturbation direction.

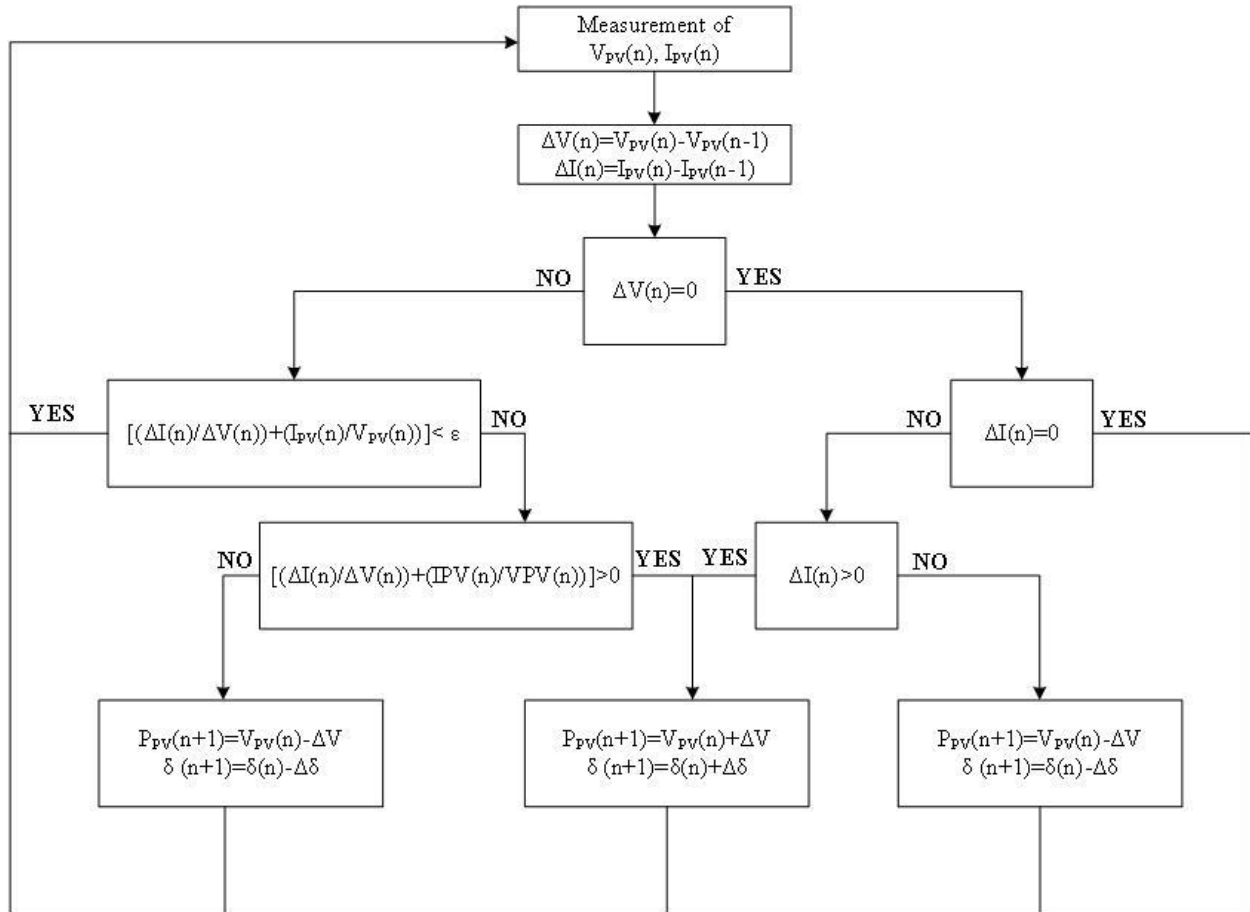


Figure 6: InC Method's flowchart

B. Perturb and observe method

P&O algorithms function by regularly adjusting (increasing or decreasing) the voltage applied to the array terminals and then comparing the photovoltaic (PV) output power with the power generated during the previous adjustment cycle. This process allows the algorithm to track and optimize the power output of the photovoltaic system efficiently. The rate of change of power in relation to voltage (dP/dV_{PV}) serves as the basis for the feedback mechanism used by the PV array control system. The control system continues to move the operating point of the PV array in the same direction as the operating voltage changes and the power output rises ($dP/dV_{PV}>0$)[9]. On the other hand, the operating point is moved in the other direction if the power output drops ($dP/dV_{PV}<0$). Following perturbation cycles, this iterative process is repeated, enabling the algorithm to continuously improve the PV array's performance and maximum power generation efficiency. Each MPPT (Maximum Power Point Tracking) cycle causes the array terminal voltage to fluctuate, which is a serious problem that the P&O algorithms frequently run into. The output power, therefore, begins to oscillate about the maximum value when the PV system hits the Maximum Power Point (MPP). As well as under quickly changing atmospheric circumstances, this oscillation phenomenon also happens in situations of steady or slowly variable atmospheric conditions [10]. Due to these oscillations, the total amount of power produced by the PV system decreases, which has an impact on the MPPT process's effectiveness.

The conventional P&O methodology (P&Oa), the improved P&O technique (P&Ob), and the three-point P&O approach (P&Oc) are all examined in this study. The perturbations applied to the photovoltaic operating point in the traditional P&O approach (P&Oa) have a defined magnitude, as shown in Figure 7. The amount of disturbance ($\Delta\delta$) for our investigation is set at 0.35% of the PV array's V_{OC} (Voltage at Open Circuit)[11]. By averaging many samples of the array power, the improved P&O approach (P&Ob) dynamically adjusts the magnitude of the perturbation. By analyzing the MOV (Mean Output Voltage) and computing the parameter $a(n)$ based on the data

shown in Figure 8, this dynamic adjustment is accomplished. To determine the direction of the disturbance, the three-point weight comparison approach (P&Oc) compares the PV output power at three separate points along the P-V (Power-Voltage) curve. This method's fundamental component, the parameter M, which is illustrated in Figure 9, directs the choice of perturbation direction. The goal of this research is to obtain insights into the efficacy and efficiency of these three P&O algorithms in improving the power output of the solar system under diverse scenarios. As each of the three methods depends on three distinct points on the P-V (Power-Voltage) curve, measuring the PV array voltage (V_{PV}) and current (I_{PV}) is crucial. These algorithms demonstrate their effectiveness in optimizing the power output of photovoltaic systems through accurate V_{PV} and I_{PV} readings. They achieve this by evaluating the perturbation direction and amplitude. The process involves working with three key points: point B, which is a perturbed version of point A, followed by point C, a doubly perturbed point situated in the opposite direction of B. Finally, point A represents the PV operating voltage adjustment reference.

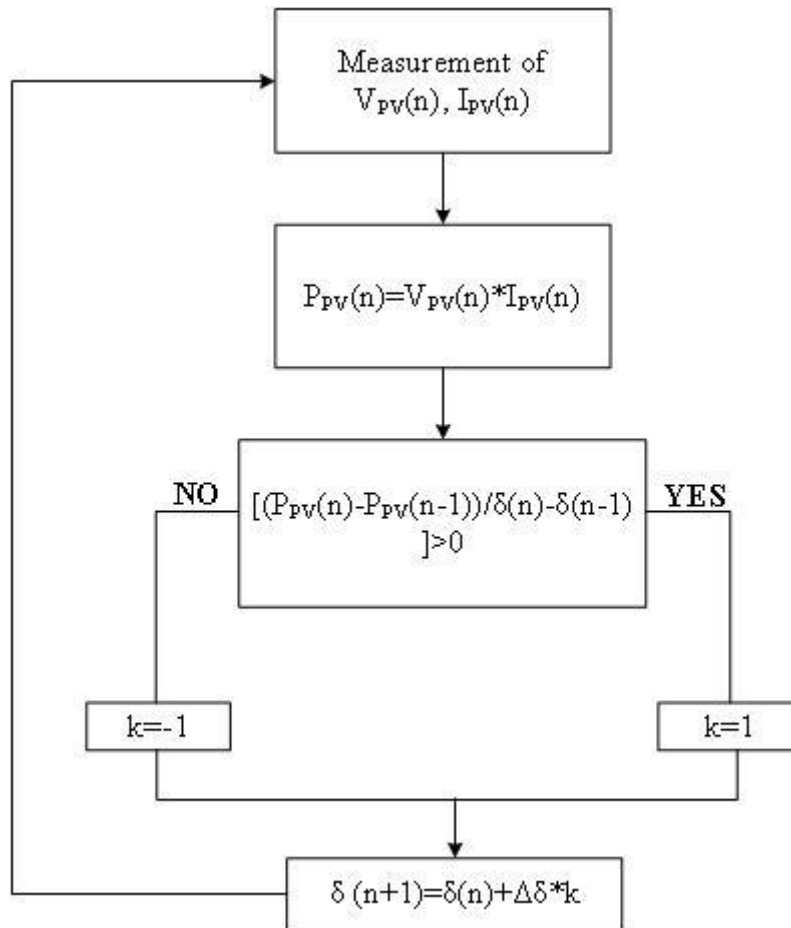


Figure 7: P&Oa method's flow chart

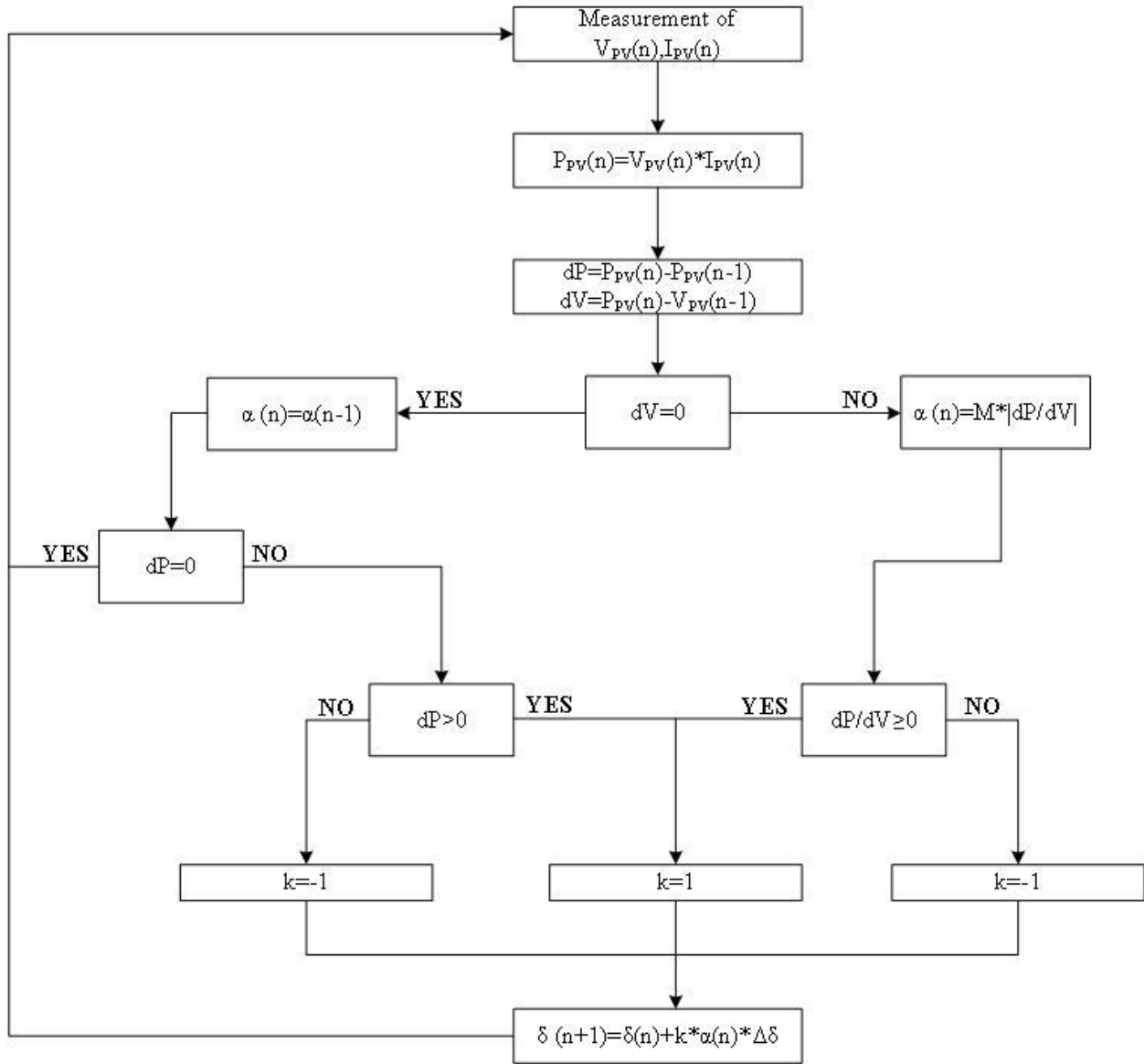


Figure 8: P&Ob method's flow chart

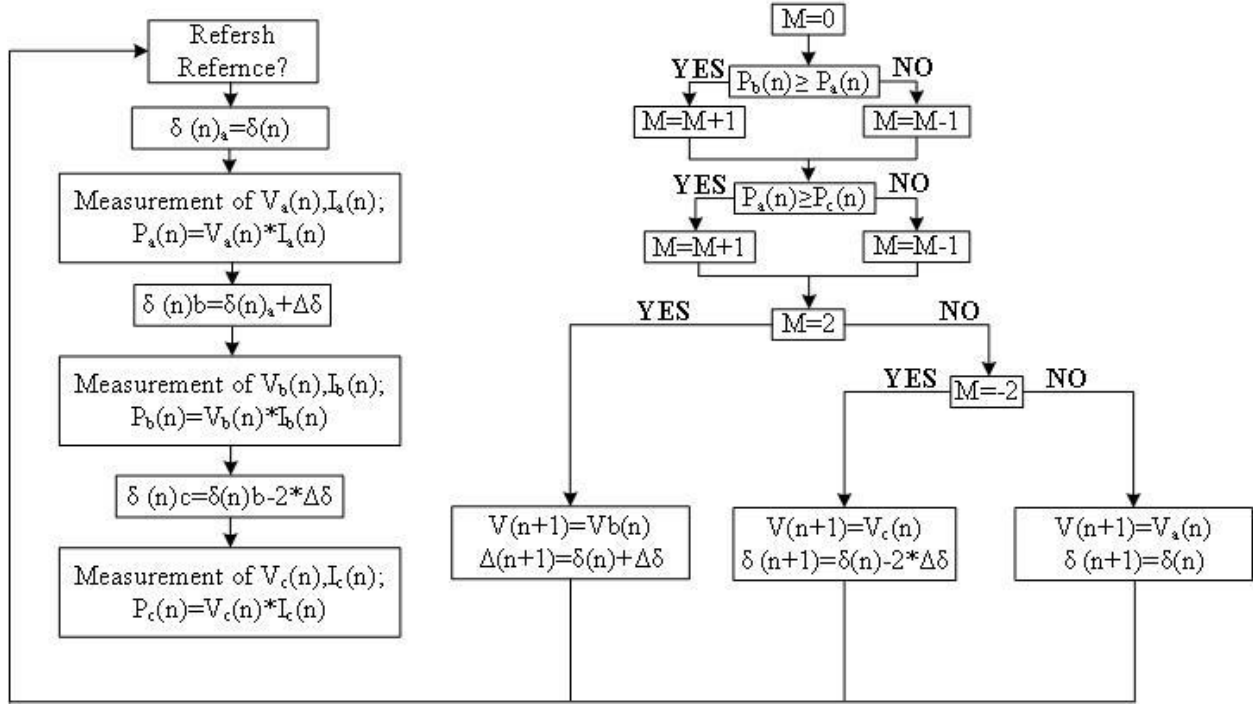


Figure 9: P&Oc method's flow chart

C. Fuzzy logic controller method

Fuzzy logic control is one of the most influential and fruitful applications of fuzzy logic theory today, thanks in large part to advancements in microelectronic technology. When provided as (IF-THEN) statements, language control rules may be effectively automated into control strategies using FLC, which are based on fuzzy logic principles[11]. Fuzzy logic control has become widely used in many other sectors and disciplines as a result of these developments, and it has proven to be a useful tool for improving control systems and decision-making procedures.

The FLC has two inputs: error E and change of error CE.

$$E(k) = \frac{P(k) - P(k-1)}{V(k) - V(k-1)} \quad (4)$$

$$CE(k) = E(k) - E(k-1) \quad (5)$$

P(k): Stands for the output power of a photovoltaic panel at sampling time k. It represents the electrical energy that the PV panel generated at a certain moment.

V(k): Specifies the output voltage of the Photovoltaic panel at sampling instant k. It displays the electrical voltage that the PV panel produced at a certain moment.

gE: This is the fuzzy logic controller's input scaling factor. It is used to scale the input variable for the electrical power of the PV panel (P(k)).

gCD: This is the fuzzy logic controller's input scaling factor. It is used to scale the input variable for the voltage (V(k)) of the PV panel.

gdD: This is the Defuzzification gain, which is an output scaling factor for the fuzzy logic controller. It is used to scale the output variable (dD) of the fuzzy process.

dd: The output of the fuzzy procedure is shown. Given the input variables (P(k), V(k)) and the predefined fuzzy rules, it probably represents the control signal or decision made by the fuzzy logic controller in this case.

The fuzzy rules and inference-engine, the de-fuzzification building block, and the fuzzification building block are the three functional building blocks that make up the fuzzy logic controller.

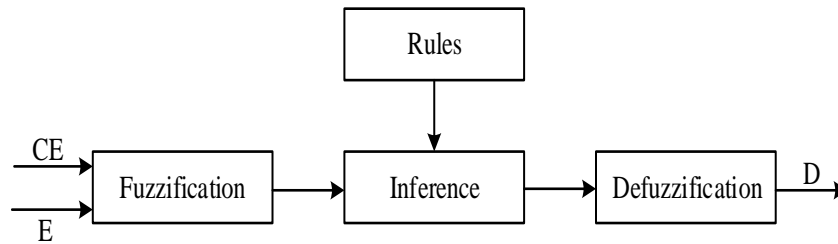
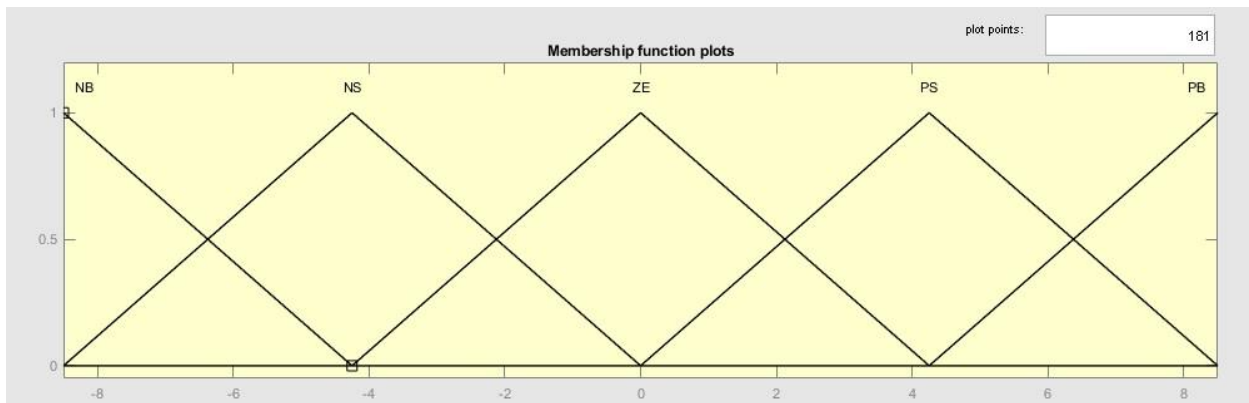


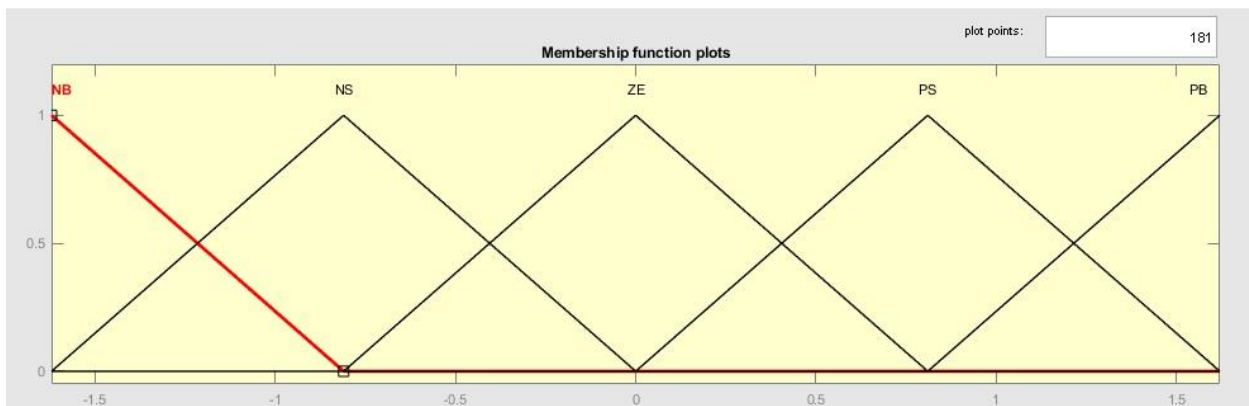
Figure 10: Fuzzy Logic Controller Block

1. Fuzzification

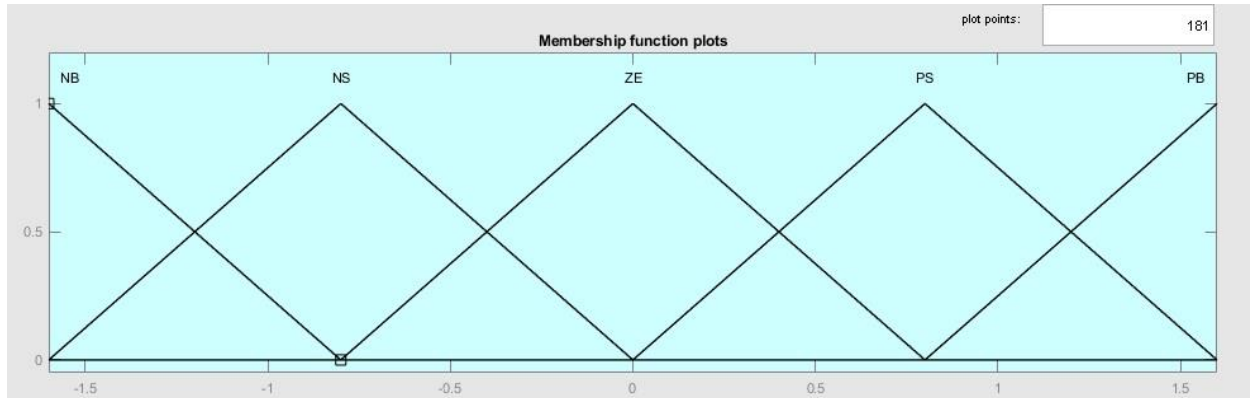
The fuzzy process demands that each variable that is used in the description of the control rules be stated in terms of fuzzy set notations in addition to their respective linguistic names. This is a requirement that must be met before the fuzzy process can be implemented. Figure 11 depicts the membership functions for the output variable $dD(k)$, as well as the membership functions for the input variables $E(k)$ and $CE(k)$. Each membership function is given one of the five fuzzy sets, which are denoted by the acronyms PB (Positive Big), PS (Positive Small), ZE (Zero), NS (Negative Small), and NB (Negative Big).



(a)



(b)



(c)

Figure 11: Membership Functions

2. Fuzzy rule and inference engine

The FI system is the basis for fuzzy logic controllers and acts as their foundation. The process of fuzzy inference refers to the use of FL in order to transform a given input into an output. Following this, a framework for decision-making is provided by the mapping. The inference method of the Mamdani type that has been offered makes an attempt to bring the error function (represented by E in formula 4) down to zero. Take into consideration the two situations that are listed below [12]:

Case. I: The working point has a positive value and is located to the left of the MPP. The working point shifts in the direction of the MPP if the change in error CE is positive. The opposite occurs when CE is negative.

Case. II: The working point is to the right of the MPP because E is negative. In this situation, the working point goes back toward the MPP if CE is negative and forward if CE is positive.

From there, we summarize this process of thinking as a series of fuzzy IF-THEN rules in Table 1.

Table 1: Rule Table

| Fuzzy Rule | | ErrorE(k) | | | | |
|-----------------------------|----|-----------|----|----|----|----|
| | | NB | NS | ZE | PS | PB |
| Change in Error CE(k) | PB | ZE | ZE | PS | PS | PB |
| | PS | NS | ZE | ZE | PS | PS |
| | ZE | NS | ZE | ZE | ZE | PS |
| | NS | NS | NS | ZE | ZE | PS |
| | NB | NB | NS | NS | ZE | ZE |

3. De-fuzzification

Calculating the crisp output of the FLC is part of the defuzzification process. It demonstrates how to convert a space of FL statements that correspond to inferred output into a non-fuzzy control action. This research used the COG Defuzzifier, the most widely utilized defuzzifier [13].

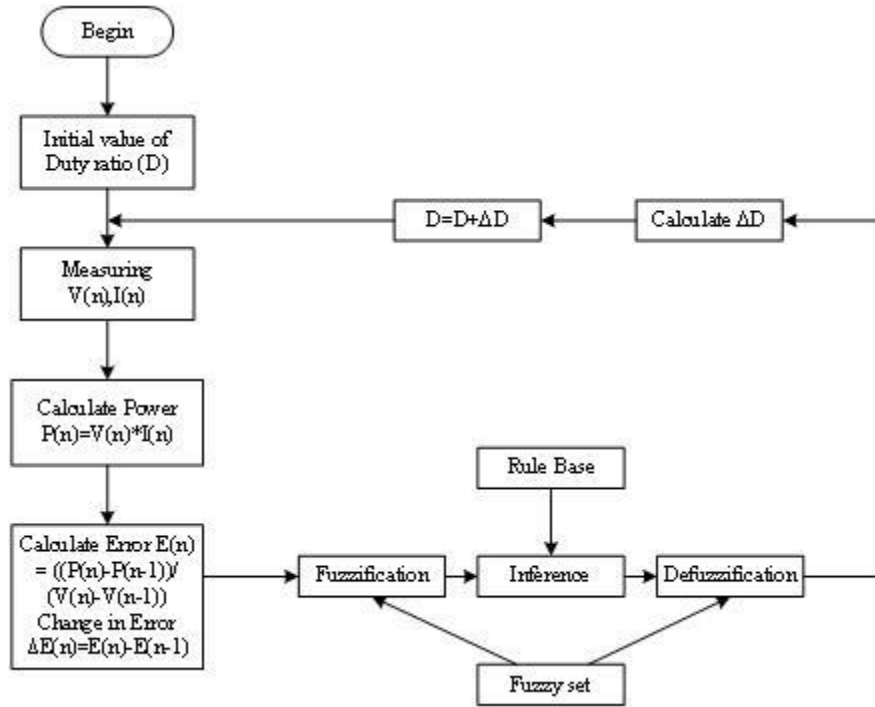


Figure 12: FLC method's flow chart

SIMULATION RESULT

The Matlab/Simulink implementation of the three MPPT algorithms under consideration in this comparative research. The 1Soltech 1STH-250-WH module was chosen as the PV module for this investigation since it can 250 watts of output power should be produced. The specifications of the photovoltaic parts are listed in correspondingly, table 2. Equation (1) is used to model the output characteristics of a PV array under various solar radiation conditions (1000W/m², 800W/m², and 600W/m²) and at a constant ambient temperature maintained at 25°C. As seen in Figures 2 and 3, a PV array has nonlinear properties, and since a PV generating system can only operate at one specific point to provide its maximum output power, MPPT technologies must be used instead.

Table 2: Parameters of the Solar (PV) array

| Parameters | Values |
|------------------------------------|---------------|
| Maximum Power (P_{max}) | 250 W |
| Voltage at MPP (V_{MPP}) | 30.7 V |
| Current at MPP (I_{MPP}) | 8.15 A |
| Open Circuit Voltage (V_{oc}) | 37.3 V |
| Short Circuit Voltage (I_{sc}) | 8.66 A |
| Cells Per Module (N_{cell}) | 60 |
| Shunt Resistance (R_{sh}) | 224.1886 ohms |
| Series Resistance (R_s) | 0.23724 ohms |

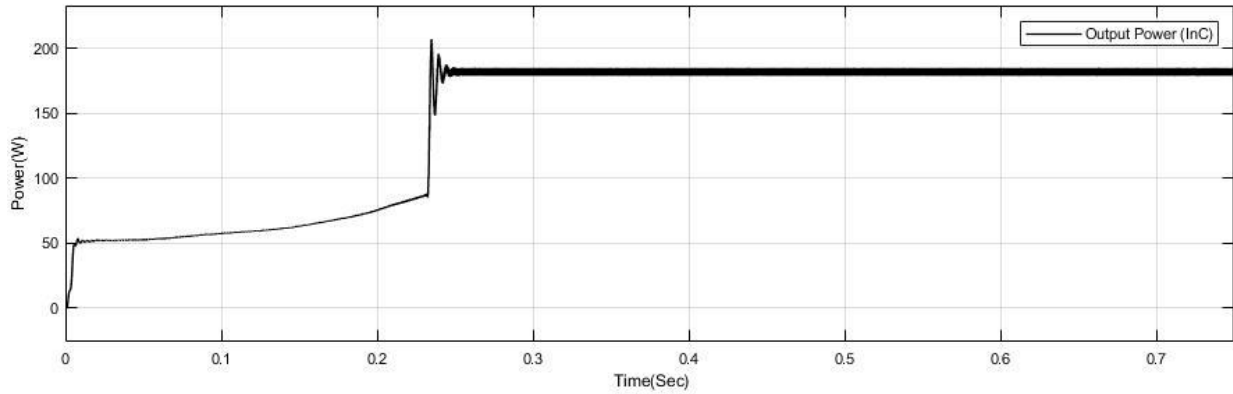


Figure 13: Output Power of Incremental Conduction at 1000W/m² and constant temperature(25°C)

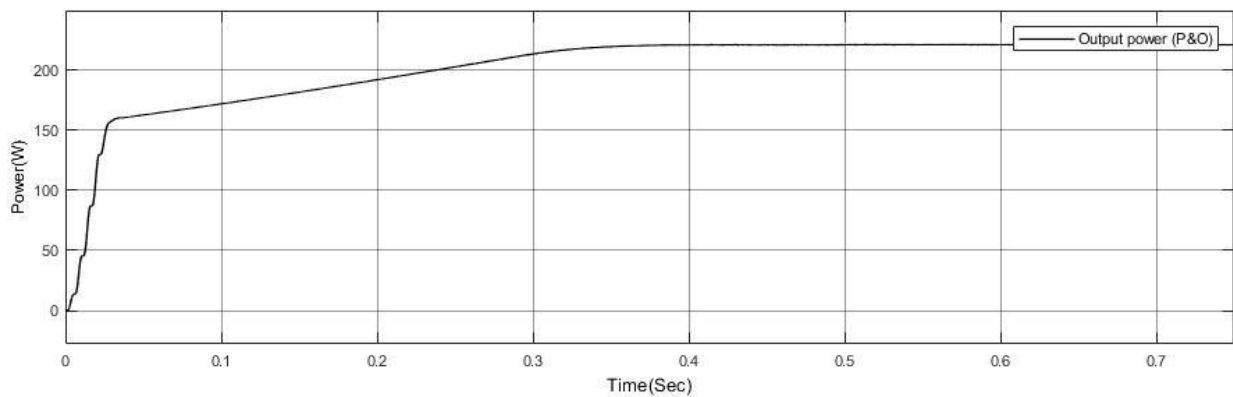


Figure 14: Output Power of Perturbation and observation(P&O) at 1000W/m² and constant temperature(25°C)

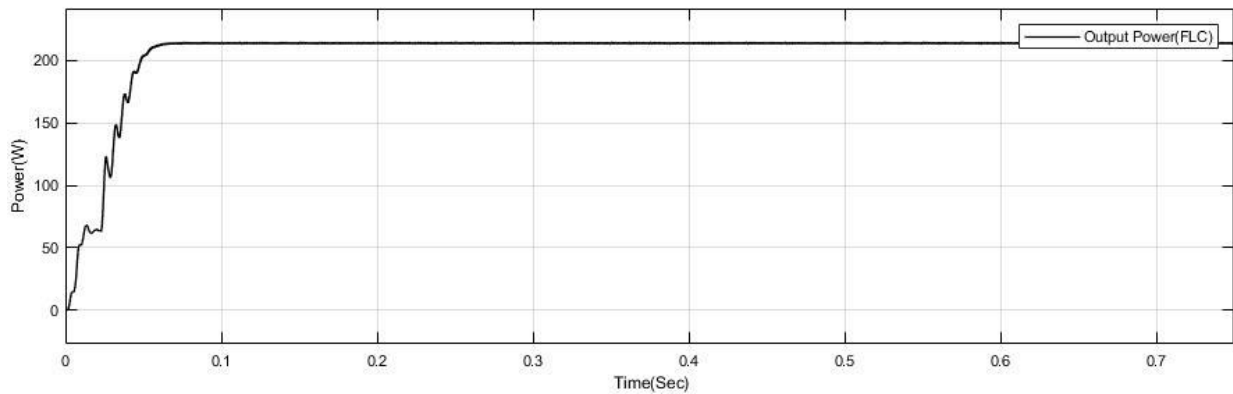


Figure 15: Output Power of Fuzzy logic controller at 1000W/m² and constant temperature(25°C)

First, the three MPPT's performance is tested under typical conditions, and then it is compared in terms of efficiency tracking. The following equation yields the efficiency tracking [7]:

$$\eta_T = \frac{\int_{t_2}^{t_1} P \cdot dt}{\int_{t_2}^{t_1} P_{\max} \cdot dt} \quad (6)$$

P is the output power of the array, and Pmax is the theoretical maximum array power, where t₁ and t₂ are the times at which the system starts up and shuts down.

Table 3: Performance Evaluation of Various MPPT Techniques in a Standard Environment

| MPPT Method | 1000W/m ² ,25°C | |
|-------------|----------------------------|----------------|
| | Response time (s) | Efficiency (%) |
| P&O | 0.53 | 85.2 |
| InC | 0.235 | 82.92 |
| FLC | 0.232 | 86 |

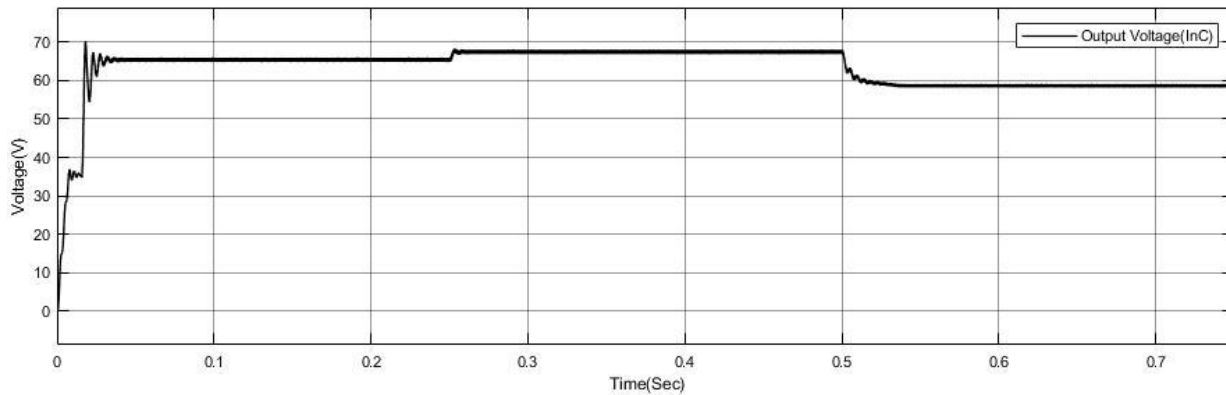


Figure 16.a: Output Voltage (InC) of PV for various irradiance and constant temperature 25°C

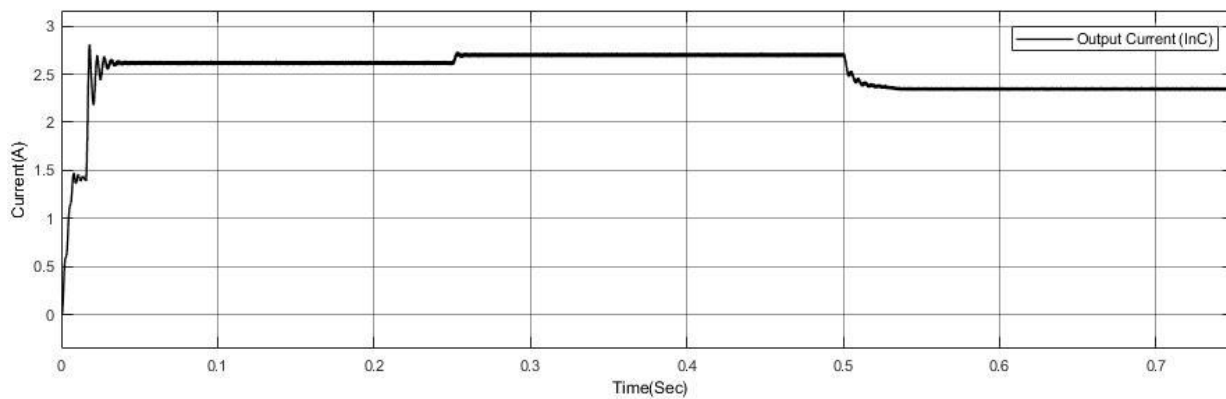


Figure 16.b: Output Current (InC) of PV for various irradiance and constant temperature 25°C

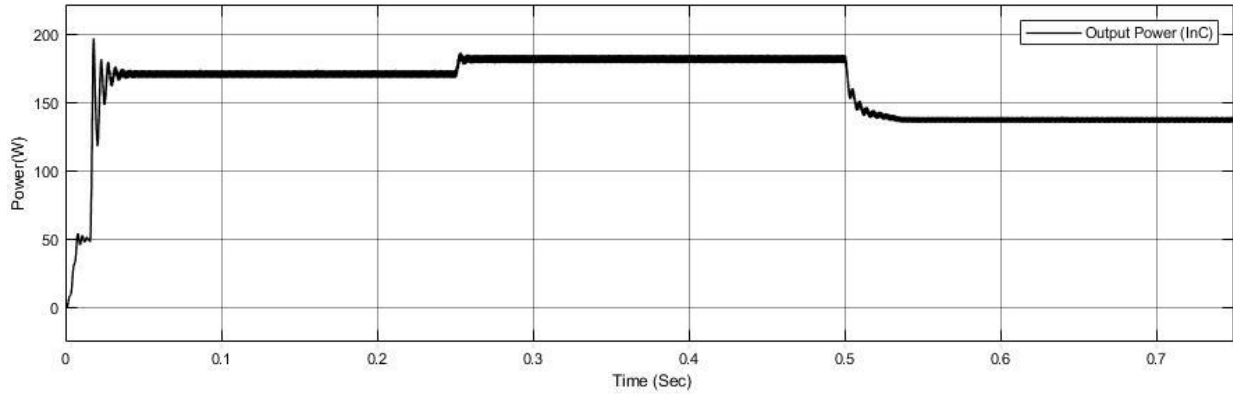


Figure 16.c: Output Power (InC) of PV for various irradiance and constant temperature 25°C

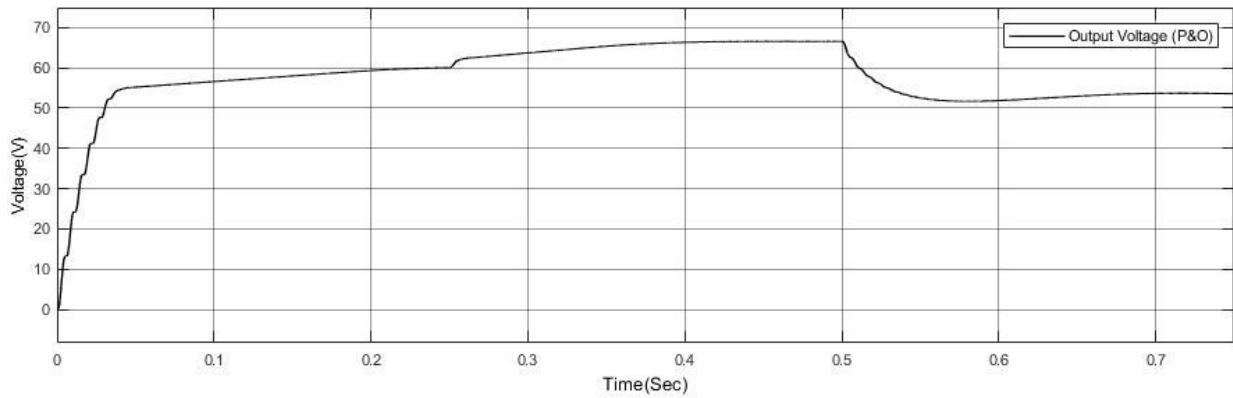


Figure 17.a: Output Voltage (P&O) of PV for various irradiance and constant temperature 25°C

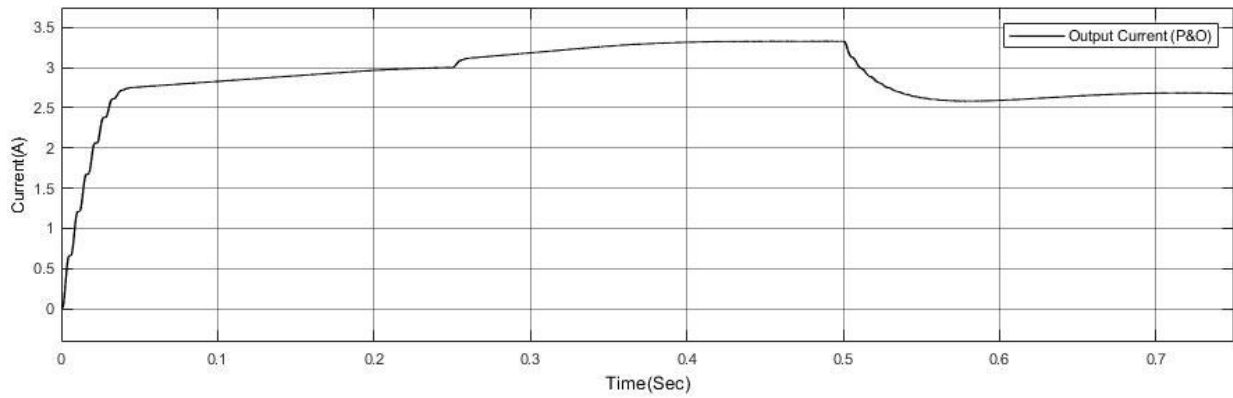


Figure 17.b: Output Current (P&O) of PV for various irradiance and constant temperature 25°C

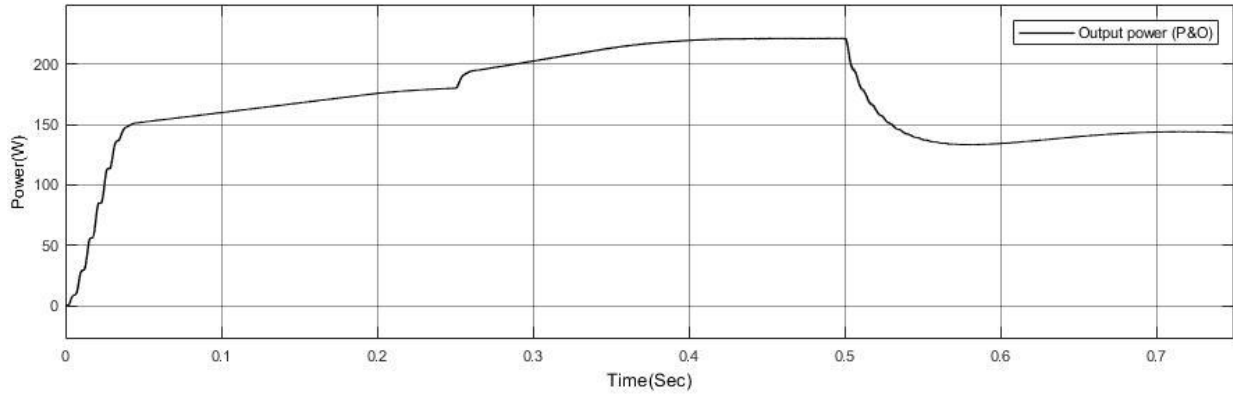


Figure 17.c: Output Power (P&O) of PV for various irradiance and constant temperature 25°C

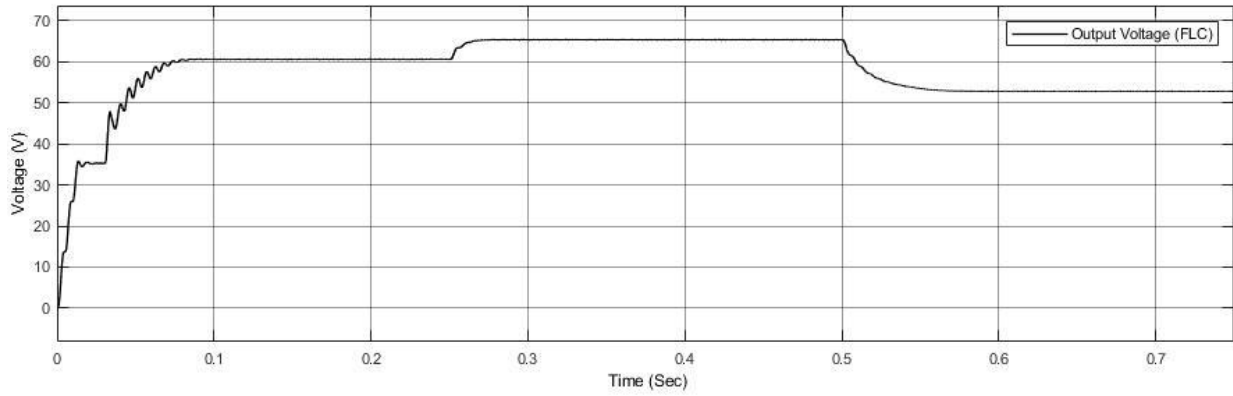


Figure 18.a: Output Voltage (FLC) of PV for various irradiance and constant temperature 25°C

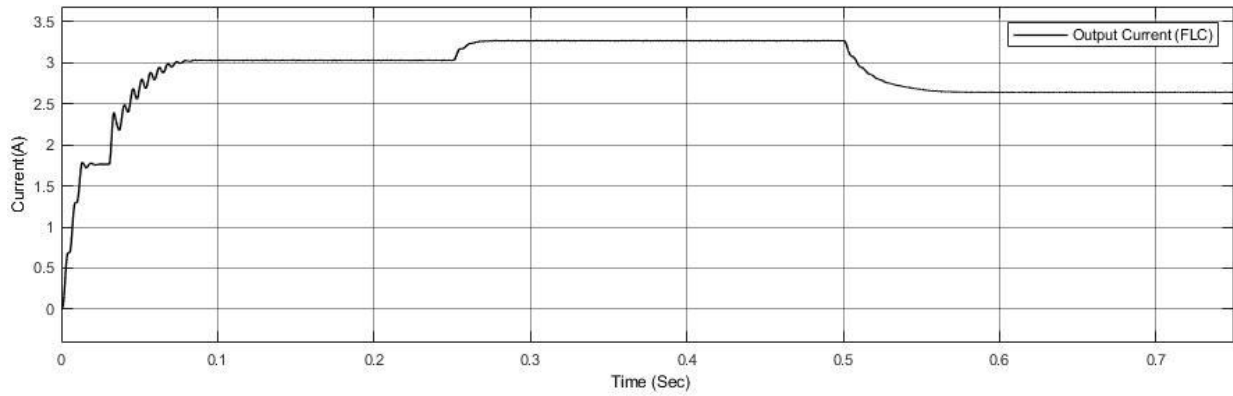


Figure 18.b: Output Current (FLC) of PV for various irradiance and constant temperature 25°C

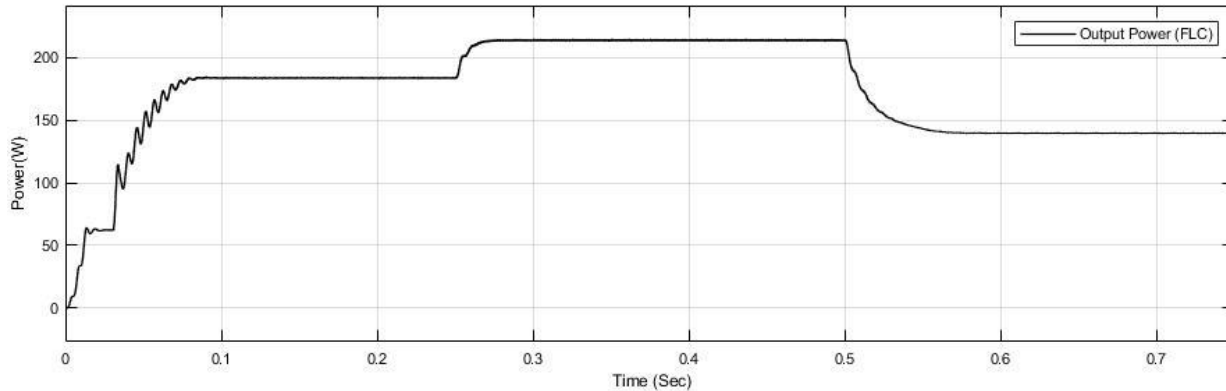


Figure 18.c: Output Power (FLC) of PV for various irradiance and constant temperature 25°C

Figs.13 to 15 illustrate, accordingly, the output solar panel power using the three MPPT algorithms at 1000W/m² and 25°C. It is found that the response times required by the conventional ways, P&O and INC, to contact the MPP are much longer than those required by the clever approach, FLC. Table 3 provides a comparison of the three MPPTs under typical environmental conditions. We alter the irradiation to show how our system behaves under actual conditions. Figures 16.a, 16.b, 16.c, 17.a, 17.b, 17.c, and 18.a, 18.b, 18.c show the output voltage, current, power respectively for various MPPT approaches and for various irradiance and fixed temperature values. As the irradiance increases (from 800W/m² to 1000W/m²), it is demonstrated that the three MPPT studies evaluate the proper power simultaneously. However, the intelligent techniques (FLC) are quicker than the conventional methods when the irradiance is reduced (thus from 1000W/m² to 600W/m²).

V. CONCLUSION

This research includes an analysis of several traditional and intelligent Maximum PowerPoint Tracking (MPPT) techniques. The objective was to evaluate how well they performed in terms of efficiency and response time. The intelligent strategies, in particular, the Fuzzy Logic Controller (FLC) approach, outperformed the other methods that were assessed. The findings demonstrated that the FLC-based MPPT algorithm provided an outstanding solution, giving the maximum efficiency and response time in steady-state settings as well as when exposed to variable irradiation levels. These findings highlight the potential of intelligent techniques such as FLC, for optimizing the power output of photovoltaic systems and overcoming challenges posed by changing environmental conditions. By adopting these advanced algorithms, solar power systems can operate more efficiently and effectively, leading to enhanced energy harvesting capabilities.

References

- [1] H. Bhati and L. Gidwani, "Solar Energy Application: A Decade Review," *Int. Res. J. Eng. Technol.*, pp. 1489–1507, 2023, [Online]. Available: www.irjet.net
- [2] A. Mohapatra, B. Nayak, and C. Saiprakash, "Adaptive Perturb Observe MPPT for PV System with Experimental Validation," *1st IEEE Int. Conf. Sustain. Energy Technol. Syst. ICSETS 2019*, no. 1, pp. 257–261, 2019, doi: 10.1109/ICSETS.2019.8744819.
- [3] A. Saleh, K. S. Faiqotul Azmi, T. Hardianto, and W. Hadi, "Comparison of MPPT fuzzy logic controller based on perturb and observe (P&O) and incremental conductance (INC) algorithm on buck-boost converter," *Proc. - 2018 2nd Int. Conf. Electr. Eng. Informatics Towar. Most Effic. W. Mak. Deal. with Futur. Electr. Power Syst. Big Data Anal. ICon EEI 2018*, no. October, pp. 154–158, 2018, doi: 10.1109/ICon-EEI.2018.8784324.
- [4] H. Bhati, "Solar PV System Based on Fuzzy Logic MPPT Algorithm," *J. Emerg. Technol. Innov. Res.*, vol. 10, no. 4, pp. m322–m335, 2023, doi: <http://doi.org/10.1729/Journal.34008>.
- [5] J. Kumar, B. Rathor, and P. Bahrani, "Fuzzy and P amp; O MPPT techniques for stabilized the efficiency of solar PV system," *2018 Int. Conf. Comput. Power Commun. Technol. GUCON 2018*, no. Dc, pp. 259–264, 2019, doi: 10.1109/GUCON.2018.8674909.
- [6] K. Jain, M. Gupta, and A. Kumar Bohre, "Implementation and Comparative Analysis of PO and INC MPPT Method for PV System," *India Int. Conf. Power Electron. IICPE*, vol. 2018-December, pp. 1–6, 2018, doi: 10.1109/IICPE.2018.8709519.
- [7] Shalini, "Simulation and Modelling of MPPT based PV System Connected with Boost Converter," *2020 IEEE Pune Sect. Int. Conf.*

PuneCon 2020, no. 1, pp. 83–87, 2020, doi: 10.1109/PuneCon50868.2020.9362452.

- [8] C. H. Hussaian Basha and C. Rani, “Performance Analysis of MPPT Techniques for Dynamic Irradiation Condition of Solar PV,” *Int. J. Fuzzy Syst.*, vol. 22, no. 8, pp. 2577–2598, 2020, doi: 10.1007/s40815-020-00974-y.
- [9] M. L. Azad, S. Das, P. Kumar Sadhu, B. Satpati, A. Gupta, and P. Arvind, “P&O algorithm based MPPT technique for solar PV system under different weather conditions,” *Proc. IEEE Int. Conf. Circuit, Power Comput. Technol. ICCPCT 2017*, pp. 0–4, 2017, doi: 10.1109/ICCPCT.2017.8074225.
- [10] R. Benkercha, S. Moulahoum, and I. Colak, “Modelling of fuzzy logic controller of a maximum power point tracker based on artificial neural network,” *Proc. - 16th IEEE Int. Conf. Mach. Learn. Appl. ICMLA 2017*, vol. 2017-Decem, pp. 485–492, 2017, doi: 10.1109/ICMLA.2017.0-114.
- [11] J. P. Gaubert, L. Rahmani, and S. Mekhilef, “Experimental verification of P & O MPPT algorithm with direct control based on Fuzzy logic control using CUK converter,” 2015, doi: 10.1002/etep.
- [12] A. Omar, M. Waweru, R. R.-T. I. J. of, and undefined 2015, “A literature survey: Fuzzy logic and qualitative performance evaluation of supply chain management,” *Theijes.Com*, pp. 56–63, 2015, [Online]. Available: <http://www.theijes.com/papers/v4-i5/Version-1/G0451056063.pdf>
- [13] N. Jeddi and L. El Amraoui Ouni, “Comparative study of MPPT techniques for PV control systems,” *2014 Int. Conf. Electr. Sci. Technol. Maghreb, Cist. 2014*, no. May, 2014, doi: 10.1109/CISTEM.2014.7077034.